Current Density Maps, Magnetizability, and Nuclear Magnetic Shielding Tensors for Anthracene, Phenanthrene, and Triphenylene

Andrea Ligabue, Ugo Pincelli, Paolo Lazzeretti,* and Riccardo Zanasi

Contribution from the Dipartimento di Chimica dell'Università di Modena, via G. Campi 183, 41100 Modena, Italy, and Dipartimento di Chimica, Università degli Studi di Salerno, via S. Allende, 84081 Baronissi (SA), Italy

Received January 7, 1999. Revised Manuscript Received March 29, 1999

Abstract: Ab initio magnetically induced π-electron (first-order) current density maps and second-order magnetic properties, i.e., magnetizabilies, proton, and ^{13}C magnetic shielding tensors, calculated at coupled Hartree−Fock level of theory by means of the continuous transformation of origin of the current density method (CTOCD), are presented for a series of polycyclic aromatic hydrocarbons. The reliability of the current density maps is documented by the nice agreement between theoretical values for principal values of magnetizabilities and proton magnetic shieldings and corresponding experimental data presently available. For all three of the molecules, the π-electron current flows mainly on the external circuit of carbon atoms. Other intense circulations localized on a single ring take place over the central hexagon of anthracene and, on the contrary, on the external hexagons of phenanthrene and triphenylene. In light of the results obtained in the present work, e.g., taking advantage of high quality current density maps, important details of the ring current model for the molecules under study can be reexamined. Eventually, it is shown that the fundamental information which can be gained from knowledge of the principal components of the magnetic response tensors is easily accessible by means of the CTOCD computational method adopted here.

Introduction

The magnetic properties of aromatic hydrocarbons, i.e., NMR shielding constants and magnetizabilities, are commonly interpreted on the basis of the well-known ring current model (RCM),[1−3] which dates back to the early days of quantum mechanics.[4] In 1979, 1989, and 1997 three major reviews of the "ring current concept" were published.[5−7] Nevertheless, quantum mechanical methods for the calculation of accurate electron current densities in polyatomic molecules have been proposed only quite recently.[8−10] The approaches based on Keith and Bader's distributed-origin Ansatz,[10] hereafter indicated by the acronym CTOCD (from continuous transformation of origin of current density[11]), yield reliable predictions of both the actual pattern of magnetic field induced electron current density[12−17] and molecular magnetic properties.[18−21]

The aim of the present work is 2-fold: (i) to provide a step forward in the field by reporting coupled Hartree−Fock (CHF) estimates close to the Hartree−Fock limit for a series of magnetic properties via the CTOCD scheme-in particular we attempted to evaluate accurate π-electron current density maps, theoretical magnetizabilities, and nuclear magnetic shielding tensors for anthracene (**1**), phenanthrene (**2**), and triphenylene (**3**) molecules, for which experimental principal values of the

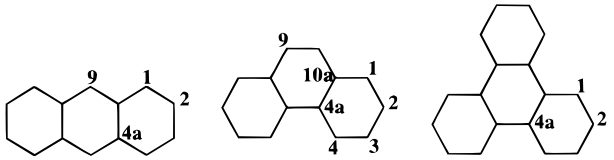

1 2 3

^{13}C magnetic shielding tensors have been recently reported;[22,23]

* Corresponding author. E-mail: lazzeret@unimo.it.

(1) Pauling, L. *J. Chem. Phys.* **1936**, *4*, 673.
(2) London, F. *J. Phys. Radium* **1937**, *8*, 397.
(3) Lonsdale, K. *Proc. R. Soc. London* **1937**, *A159*, 149.
(4) Ehrenfest, P. *Physica* **1925**, *5*, 388.
(5) Haigh, C. W.; Mallion, R. B. Ring current theories in nuclear magnetic resonance. In *Progress in Nuclear Magnetic Resonance Spectroscopy*; Emsley, J. W., Feeney, J., Sutcliffe, L. H., Eds.; Pergamon Press: Oxford, 1979; Vol. 13, Part 4, pp 303−344.
(6) Haigh, C. W.; Mallion, R. B. *Croat. Chim. Acta* **1989**, *62*, 1−26.
(7) Gomes, J. A. N. F.; Mallion, R. B. The Concept of Ring Currents. In *Concepts in Chemistry: A Contemporary Challenge*; D. H. Rouvray, Ed.; Research Studies Press: Taunton, Somerset, U.K., 1997; pp 205−253.
(8) Lazzeretti, P.; Zanasi, R. *Chem. Phys. Lett.* **1981**, *80*, 533−536.
(9) Lazzeretti, P.; Zanasi, R. *J. Chem. Phys.* **1982**, *77*, 3129−3139.
(10) Keith, T. A.; Bader, R. F. W. *Chem. Phys. Lett.* **1993**, *210*, 223−231.
(11) Lazzeretti, P.; Malagoli, M.; Zanasi, R. *Chem. Phys. Lett.* **1994**, *220*, 299−304; Coriani, S.; Lazzeretti, P.; Malagoli, M.; Zanasi, R. *Theor. Chim. Acta* **1994**, *89*, 181−192; Zanasi, R.; Lazzeretti, P.; Malagoli, M.; Piccinini, F. *J. Chem. Phys.* **1995**, *102*, 7150−7157.
(12) Bader, R. F. W.; Keith, T. A. *J. Chem. Phys.* **1993**, *99*, 3683−3693.
(13) Zanasi, R.; Fowler, P. W. *Chem. Phys. Lett.* **1995**, *238*, 270−280.
(14) Fowler, P. W.; Zanasi, R.; Cadioli, B.; Steiner, E. *Chem. Phys. Lett.* **1996**, *251*, 132−140.
(15) Steiner, E.; Fowler, P. W. *Int. J. Quantum Chem.* **1996**, *60*, 609−616.
(16) Zanasi, R.; Lazzeretti, P. *Mol. Phys.* **1997**, *92*, 609−617.
(17) Fowler, P. W.; Steiner, E.; Cadioli, B.; Zanasi, R. *J. Phys. Chem.* **1998**, *102*, 7297.
(18) Lazzeretti, P.; Malagoli, M.; Zanasi, R. *J. Chem. Phys.* **1995**, *102*, 9619−9625.
(19) Zanasi, R. *J. Chem. Phys.* **1996**, *105*, 1460−1469.
(20) Lazzeretti, P.; Zanasi, R. *Int. J. Quantum Chem.* **1996**, *60*, 249−259.
(21) Zanasi, R.; Lazzeretti, P.; Fowler, P. W. *Chem. Phys. Lett.* **1997**, *278*, 251−255.
(22) Tarroni, R.; Zannoni, C. *J. Phys. Chem.* **1996**, *100*, 17157−17165.
(23) Soderquist, A.; Hughes, C. D.; Horton, W. J.; Facelli, J. C.; Grant, D. M. *J. Am. Chem. Soc.* **1992**, *114*, 2826−2832.

10.1021/ja9900656 CCC: $18.00
Published on Web 05/27/1999

(ii) to document the practicality of the CTOCD method for the understanding of magnetic response of important polycyclic aromatic hydrocarbons, customarily interpreted on the basis of the RCM, to gauge the usefulness of the model for these molecular systems.

Beside these motivations, knowledge of the components of magnetizability and of nuclear magnetic shielding tensors provides valuable information on the electronic structure of the molecules under investigation. In particular, the magnetizability tensor of aromatic systems systematically shows an enhanced anisotropy, $\Delta\chi$, due to a very large negative component, χ_{33}, perpendicular to the molecular plane. This is explained in terms of intense current density induced by a perpendicular magnetic field in the mobile π-electron cloud. Accordingly, the value of $\Delta\chi$ can be related to the degree of electron delocalization, providing a hallmark for the aromatic character of a molecule.[24,25]

The principal values of the ^{13}C magnetic shielding tensor in aromatic systems possess quite peculiar features. The largest principal value, σ_{11}, corresponds to an axis perpendicular to the molecular plane and falls within the aliphatic NMR spectral region.[26,27] The smaller of the two in-plane principal components, σ_{33}, is negative, and π-electrons play a major role in determining its size.[26] Interestingly enough, the σ_{22} component is useful to distinguish a carbon nucleus belonging to a C−H bond from that of bridgehead carbon, which is characterized by a smaller value.[23]

Also, the principal values of the proton magnetic shielding tensors of aromatic molecules furnish essential information. The smallest principal component, σ_{33}, corresponds to the direction perpendicular to the molecular plane, which is also related to the effect of the circulation induced in the π-electron cloud by a perpendicular magnetic field. Consequently, this feature is connected with the anisotropy of the magnetizability tensor and with the aromatic character of a molecule.[24,25] The other in-plane principal values do not exceed the aliphatic NMR spectral region.[26]

Computational Details

All calculations of magnetic-field-induced first-order current density and second-order magnetic properties were carried out at the uncorrelated SCF and CHF levels using the SYSMO package.[28]

Complete optimization of molecular geometries was performed at the Hartree−Fock level of accuracy with the 6-311G standard Gaussian basis set and the default procedures and parameters of GAUSSIAN94 system of programs.[30] Symmetry-constrained planar geometries (D_{2h} for anthracene, C_{2v} for phenanthrene, and D_{3h} for triphenylene) have been adopted.

Magnetizability, χ, carbon and proton nuclear shieldings σ^C and σ^H were calculated by integration of current densities obtained by two theoretical schemes that differ only in the way they handle the well-known problem of gauge dependence of computed magnetic properties, i.e., two different criteria have been adopted to choose the origin: within the CTOCD-DZ method the origin is coincident with the point itself, which makes the diamagnetic contribution to the induced current density identically vanish; within the CTOCD-PZ method the origin is determined for each point in such a way that the transverse component of the paramagnetic induced current is annihilated.

The details of CTOCD-DZ and CTOCD-PZ techniques, the fundamental quantum mechanical constraints for charge−current conservation that they fulfill, their relation to the methods proposed by Keith and Bader[10] and Geertsen,[29] and their performance in test cases have been described at length elsewhere.[11,19]

A variant of each method, which greatly improves calculated nuclear magnetic shieldings, is obtained by shifting the origin of the current density vector toward the nearest nucleus for points close to nuclei, as suggested originally by Keith and Bader within the CSDGT method.[10] These variants, indicated by the acronyms CTOCD-DZ2 and CTOCD-PZ2,[14,19] have been adopted here.

All calculations of current density and magnetic properties were carried out with the (9s5p2d/5s2p) primitive Gaussian basis set contracted to [5s4p1d/3s1p]. At all events, it has been pointed out[15] that the quality of the current density plots obtained by using CTOCD approaches is not significantly dependent on basis set size: the main features of the current flow, e.g., location and phase portrait of singular points, are virtually unaffected by basis set changes. In fact, the accurate prediction of magnetizability and magnetic shielding constants usually requires carefully tailored basis sets, which turns out to be an expensive restriction when the coupled Hartree−Fock (CHF) common origin (CO) procedure is employed. Adopting distributed-origin methods, as done here, brings in the fundamental advantage that a relatively modest basis set can be used to obtain high quality predictions, in particular when the CTOCD-PZ2 procedure is applied to evaluate nuclear magnetic shieldings.[19] Accordingly, on the basis of previous experience,[11,13,14,19,21] the results presented in this study are expected to be good and are rather useful to rationalize trends and to provide some firm conclusions.

Results and Discussion

Current Density Maps. Maps of the current density, induced within the π-electron cloud by an external, uniform magnetic field, are presented in Figures 1−3, respectively, for anthracene, phenanthrene, and triphenylene. Each figure shows the magnitude and direction of the current density flow (normalized to a perpendicular magnetic field flux $\boldsymbol{B}$ of magnitude 1 au) evaluated at the height of 1 bohr above the molecular plane, pointing out of the plane of the paper (so that diamagnetic circulation is clockwise).

The current density map for anthracene is illustrated in Figure 1. The essential features of theoretical vector field observed in this picture are the same as that appearing in Figure 6 of ref 15, which reported analogous investigations for the first time: intense diamagnetic circulation takes place about the peripheral carbon skeleton, in accord with the ring current model. However,

(24) Labarre, J.-F.; Crasnier, F. Top. Curr. Chem. **1971**, *24*, 33.
(25) Mallion, R. B. *Pure Appl. Chem.* **1980**, *52*, 1541.
(26) Lazzeretti, P.; Malagoli, M.; Zanasi, R. *J. Mol. Struct. (THEOCHEM)* **1991**, 234, 127−145.
(27) Fleischer, U.; Kutzelnigg, W.; Lazzeretti, P.; Mülenkamp, V. *J. Am. Chem. Soc.* **1994**, *116*, 5298−5306.
(28) Lazzeretti, P.; Malagoli, M.; Zanasi, R. *CNR Technical Report on Project "Sistemi Informatici e Calcolo Parallelo"*; CNR: Rome, 1991; Vol, 1, p 67.
(29) Geertsen, J. *J. Chem. Phys.* **1989**, *90*, 4892−4894; *Chem. Phys. Lett.* **1991**, *179*, 479−482; **1992**, *188*, 326−331.
(30) Gaussian 94, Revision D.4, Frisch, M. J.; Trucks, G. W.; Schlegel, H. B.; Gill, P. M. W.; Johnson, B. G.; Robb, M. A.; Cheeseman, J. R.; Keith, T.; Petersson, G. A.; Montgomery, J. A.; Raghavachari, K.; Al-Laham, M. A.; Zakrzewski, V. G.; Ortiz, J. V.; Foresman, J. B.; Cioslowski, J.; Stefanov, B. B.; Nanayakkara, A.; Challacombe, M.; Peng, C. Y.; Ayala, P. Y.; Chen, W.; Wong, M. W.; Andres, J. L.; Replogle, E. S.; Gomperts, R.; Martin, R. L.; Fox, D. J.; Binkley, J. S.; Defrees, D. J.; Baker, J.; Stewart, J. P.; Head-Gordon, M.; Gonzalez, C.; Pople, J. A. Gaussian, Inc., Pittsburgh, PA, 1995.

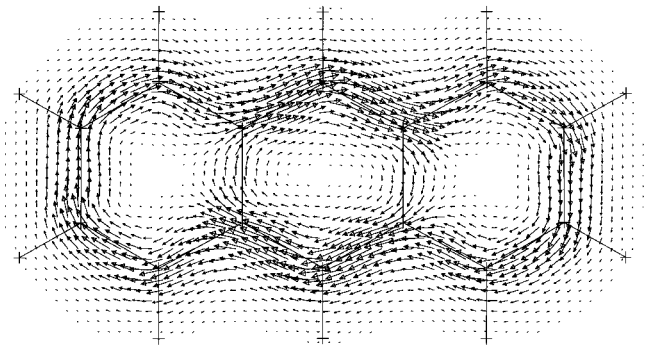

Figure 1. Diagram showing direction and magnitude of the π-current at 1 b above the molecular plane of anthracene, induced by a perpendicular magnetic field of unit magnitude pointing out of the plane of the paper. The local intensity of the vector field is proportional to the arrow length. Currents are calculated in the (9s5p2d/5s2p) basis contracted to [5s4p1d/3s1p] (see text) using the CTOCD-DZ2 approach at the optimal geometries for the 6-311G basis. Maximum magnitude of the current is 0.0995 atomic unit.

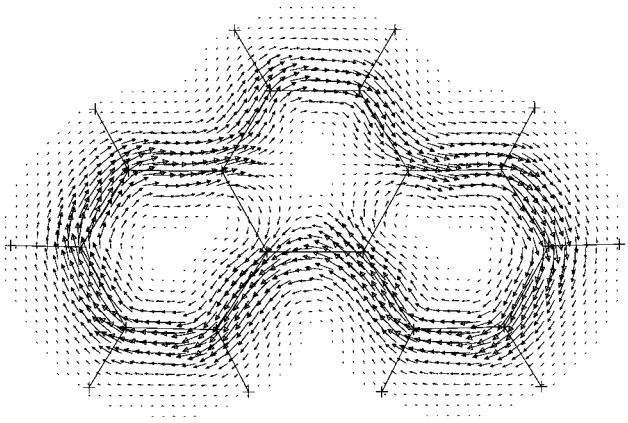

Figure 2. Same as in Figure 1 for phenanthrene. Maximum magnitude of the current is 0.0868 atomic unit.

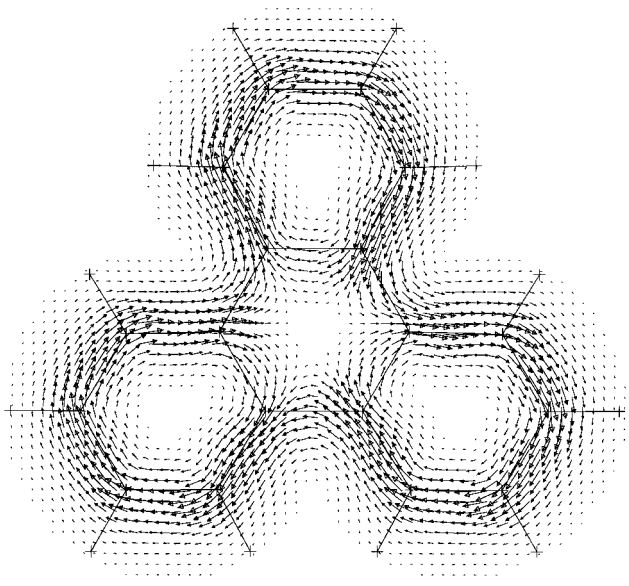

Figure 3. Same as in Figure 1 for triphenylene. Maximum magnitude of the current is 0.0835 atomic unit.

there exists a remarkable characteristic which, to some extent, conflicts with a naive application of the RCM: a strong diamagnetic current is also found all over the internal benzene ring, locally reinforcing the peripheral circulation. As a consequence, a couple of small paramagnetic vortices should appear, symmetrically placed, with their centers on the long molecular axis. Although these paramagnetic vortices are hard to see in the low resolution that necessarily characterizes the representation of a vector field used in this work, they can be spotted in the regions of molecular domain, where internal and external currents interfere destructively, on the left and on the right of the internal diamagnetic vortex.

Table 1. CTOCD-CHF Magnetizability Tensors of Anthracene, Phenanthrene, and Triphenylene[a]

	anthracene		phenanthrene		triphenylene	
component	DZ2	PZ2	DZ2	PZ2	DZ2	PZ2
χ_{11}	−1066	−1176	−1109	−1219	−1438	−1585
χ_{22}	−1215	−1337	−1180	−1292	−1438	−1585
χ_{33}	−4467	−4403	−4321	−4245	−5332	−5247
$\Delta\chi^b$	−3326	−3146	−3176	−2989	−3894	−3662
χ_{av}	−2249	−2305	−2203	−2252	−2736	−2806
exp.[d]	−2153:−2228		−2105:−2192		−2600	

[a] All quantities are in units of 10^{-30} J T^{-2} per molecule. See text for geometry and basis set. The χ_{33} component is perpendicular to the molecular plane of all three molecules. [b] Anisotropy is defined $\Delta\chi = \chi_{33} - (\chi_{11} + \chi_{22})/2$. [d] Taken from ref 36.

A rather different pattern of current flow is observed in the case of phenanthrene, a molecular system that, in the presence of a perpendicular magnetic field, is characterized by the dominance of two benzene rings comprising the biphenyl moiety. The electron circulations localized over the external rings superimpose on the one flowing all over the molecular perimeter. Accordingly, also for phenanthrene, the RCM does not provide important details of the current density vector field which are instrumental in understanding its magnetic properties. Destructive interference patterns are visible in the boundary regions between ring current flowing along the molecular perimeter and currents taking place over the external benzene fragments. These electron circulations give rise to the paramagnetic vortex which is found about the center of the internal ring.

A quite similar situation is predicted by the CTOCD method for triphenylene. Intense current densities flowing in the three external benzene rings merge, flowing along a path all over the border of carbon nuclei. Such a circulation is consistent with the usual chemical description of triphenylene as a molecule essentially characterized by three isolated benzene rings, connected by carbon−carbon bonds which are more single than double bonds. Also in this molecule a paramagnetic vortex, originating from superposition of current densities taking place over the external rings, circulates about the center of the internal hexagon.

Magnetizabilities and Shielding Constants. Magnetizabilities computed via the CHF CTOCD-DZ2 and -PZ2 methods are reported in Table 1. For all three of the molecules, the origin of the coordinate system is placed in the center of mass, the 3-principal axis of magnetizability is perpendicular to the molecular plane, the 2-direction corresponds to the long molecular axis in anthracene. Principal axis system is similarly defined in phenanthrene. It is worth recalling that CTOCD theoretical χ is independent of the origin for anthracene and triphenylene, but not for phenanthrene.[11] At any rate, the PZ values for this molecule are virtually invariant to a gauge translation.

Calculated out-of-plane χ_{33} components are much larger in absolute value than χ_{11} and χ_{22}. This fact is usually imputed to ring currents effects. However, the role of the σ electrons in concurring to the peculiar properties of benzene cannot be

Table 2. CTOCD-CHF Principal Values of the ^{13}C Magnetic Shielding Tensors in Anthracene[a]

carbon	DZ2	PZ2	exp.[b]	exp.[c]
C_1				
σ_{11}	171	170		165.8
σ_{22}	62.8	61.0		44.3
σ_{33}	−54.7	−59.5		−37.0
σ_{av}	59.7	57.2	57.7	
C_2				
σ_{11}	185	184		175.5
σ_{22}	59.7	57.2		47.4
σ_{33}	−55.2	−59.6		−41.4
σ_{av}	63.2	60.5	60.5	
C_9				
σ_{11}	164	162		155.8
σ_{22}	57.1	55.3		43.9
σ_{33}	−33.6	−38.1		−20.9
σ_{av}	62.5	59.7	59.6	
C_{4a}				
σ_{11}	202	201		191.3
σ_{22}	−4.2	−7.4		−7.7
σ_{33}	−33.6	−37.4		−21.3
σ_{av}	54.7	52.1	54.1	

[a] In ppm. See text for geometry and basis set. Absolute experimental shieldings have been obtained from the shifts reported in [b]ref 37 and [c]ref 22, using δ_C (C_6H_6) = 128.4, and $\sigma_C(C_6H_6)$ = 57.2 from ref 38.

dismissed,[31] as they drive the force for the D_{6h} structure.[32,33] The importance of strain and of the out-of-plane deformation as factors affecting the magnetic susceptibility of planar cyclic molecules has been investigated with very interesting results:[32] the nonplanarity of the carbon ring can diminish the diamagnetic susceptibility.

Within the CTOCD-PZ2 calculation, for all of the molecules studied in this work, χ_{33} components are ∼3.3 times larger than the largest in-plane component. In naphthalene the same ratio is ∼3.2.[16] However, it seems quite worth noticing that in benzene χ_{33} is only ∼2.9 times larger than $\chi_{11} = \chi_{22}$: if ring currents are responsible for this trend, their effect is apparently more significant in condensed cyclic aromatic molecules than in the archetypal six-membered aromatic system. The anisotropy $\Delta\chi = \chi_{33} - (\chi_{11} + \chi_{22})/2$ also increases noticeably with the size of the molecule. In the benzene molecule[18] the CTOCD-PZ anisotropy is -1150×10^{-30} J T^{-2} per molecule; in naphthalene[16] it is -2143×10^{-30} J T^{-2} per molecule.

CTOCD magnetic shieldings are origin idependent.[11] The results for ^{13}C shielding are reported in Tables 2−4. For all three of the cyclic molecules examined in this work, the principal 1-axis is perpendicular to the molecular plane; the orientation of 2- and 3- axes is dictated by local symmetry, and with the exception of C_9 in phenanthrene, lies within a few degrees of the C−H bond.[23]

In general, an excellent agreement between CTOCD and available experimental average magnetic shielding of the ^{13}C nucleus has been found for all of the cyclic molecules considered in this study. Only in the case of triphenylene were some little discrepancies observed for the trace of the tensor; compare the last column of Table 4. Theoretical tensor components compare less favorably with corresponding measured quantities. In any event, in the three molecules a prominent upfield shift is found for the perpendicular component, σ_{11}, in reasonable agreement with other theoretical and experimental investigations.[23] Its bulk is essentially determined by the σ-electron circulation;[23] π-electron current densities do not provide appreciable contributions.

Table 3. CTOCD-CHF Principal Values of the ^{13}C Magnetic Shielding Tensors in Phenanthrene[a]

carbon	DZ2	PZ2	exp.[b]	exp.[c]
C_1				
σ_{11}	174	172		163.6
σ_{22}	56.2	53.7		44.6
σ_{33}	−51.1	−55.5		−36.4
σ_{av}	59.7	56.7	57.1	57.6
C_4				
σ_{11}	187	186		178.6
σ_{22}	55.5	52.6		43.6
σ_{33}	−48.9	−53.4		−34.4
σ_{av}	64.5	61.7	63.0	62.6
C_9				
σ_{11}	168	166		156.6
σ_{22}	68.7	66.6		52.6
σ_{33}	−51.2	−56.1		−36.4
σ_{av}	61.8	58.8	58.7	57.6
C_2				
σ_{11}	188	187		
σ_{22}	51.5	49.2		
σ_{33}	−55.6	−60.4		
σ_{av}	61.3	58.6	59.1	
C_3				
σ_{11}	187	186		
σ_{22}	53.5	50.2		
σ_{33}	−55.5	−60.1		
σ_{av}	61.7	58.7	59.1	
C_{4a}				
σ_{11}	194	192		
σ_{22}	8.2	5.2		
σ_{33}	−35.3	−39.2		
σ_{av}	55.6	52.7	55.3	
C_{10a}				
σ_{11}	200	200		
σ_{22}	−2.0	−5.3		
σ_{33}	−34.4	−38.3		
σ_{av}	54.5	52.1	53.6	

[a] See footnote to Table 2. Absolute experimental shieldings obtained from the shifts in ref 23 as: [b]experimental liquid isotropic shifts and [c]experimental principal values.

Table 4. CTOCD-CHF Principal Values of the ^{13}C Magnetic Shielding Tensors in Triphenylene[a]

carbon	DZ2	PZ2	exp.[b]	exp.[c]
C_1				
σ_{11}	186	189		182.8
σ_{22}	54.3	52.1		45.6
σ_{33}	−48.8	−53.3		−29.4
σ_{av}	63.8	62.6	62.4	66.6
C_2				
σ_{11}	186	185		177.4
σ_{22}	52.2	49.6		48.6
σ_{33}	−56.5	−61.1		−39.4
σ_{av}	60.6	57.8	58.5	62.6
C_{4a}				
σ_{11}	190	189		186.6
σ_{22}	16.7	15.0		14.6
σ_{33}	−37.9	−41.5		−22.4
σ_{av}	56.3	54.2	55.9	59.6

[a] See footnote to Table 2. Absolute experimental shieldings obtained from the shifts in ref 23 as: [b]experimental liquid isotropic shifts and [c]experimental principal values.

In addition, it is interesting to observe that experimental chemical shifts among the perpendicular components are accounted for quite precisely; see for instance, in anthracene, the values for C_1, C_2, C_9, and C_{4a} in Table 2. Also in phenanthrene, the calculated σ_{11} values in Table 3 reproduce the observed upfield shift of C_4 relative to C_1.[23] Similar trends were found for triphenylene, see Table 4.

(31) Janoschek, R. *J. Mol. Struct.* THEOCHEM **1991**, *229*, 197−203.
(32) Ma, B.; Sulzbach, H. M.; R. B. Remington, R. B.; Schaefer, H. F., III *J. Am. Chem. Soc.* **1995**, *117*, 8392−8400.
(33) Gobbi, A.; Yamaguchi, Y.; Frenking, G.; Schaefer, H. F., III *Chem. Phys. Lett.* **1995**, *244*, 27−31.

CTOCD predictions for carbon σ_{33} systematically underestimate the corresponding experimental values. The deviations are large; compare the difference of ~22 ppm occurring for C_1 in anthracene, of ~19 ppm for C_1 in phenanthrene, and of ~24 ppm for C_1 in triphenylene found in the PZ2 calculations. These large differences have been attributed to the lack of electron correlation of conventional CHF calculations in a previous paper, where a similar pattern has been found using the LORG method.[23]

Quite significant discrepancies are also observed in the Tables for the σ_{22} component, with the noticeable exception of carbon C_{4a} for anthracene, carbon C_2, and C_{4a} of triphenylene. Remarkably enough, for phenanthrene molecule, theoretical σ_{22} components of α -carbons are quite similar, but σ_{22} is ~13−14 ppm upfield for C_9. This fact has been related to the localization of double bond in the C_9-C_{10} bond.[23]

In any case, as we emphasized above, the sum of the in-plane components is usually close to the corresponding experimental value, which might imply that the principal in-plane axes referred to here are quite differently oriented from those of ref 23. However, it is interesting to observe that significant discrepancies between experimental and theoretical in-plane components have been documented also in ref 23, where the authors state that, "At this point in time there is no experimental information on the orientation of the principal axes of the experimental ^{13}C chemical shifts in phenanthrene as this information is unavailable from powders except in cases of high symmetry....". Local deviations from perfect planarity are known to occur in cyclic condensed hydrocarbons in the solid state.[34] Present theoretical results are not sufficient to imply that slight deviations from full planarity could be locally detected also in gas phase or in solution.

Proton magnetic shielding in benzene has been discussed at length in several papers. Theoretical results obtained in most recent investigations[27,18] have probably attained the Hartree−Fock limit for the entire shielding tensor (corresponding to the molecular geometries adopted in the calculations), and provide an important reference point.

On going from olefins to benzene, or to the hypothetical cyclohexatriene, the sum of the in-plane components of proton shielding tensor stays essentially the same[27] (owing to the different orientation of the principal axis system in benzene and olefins, an analysis of this sum is more meaningful than that of the separate components). The extra deshielding of proton in benzene with respect to olefins is evident in the perpendicular component σ_{33} (theoretical values[27,18] are ~20.5), but the role of ring currents as the unique cause of this deshielding is far from being definitely ascertained.[27] In addition, delocalized ring currents induced in the σ electrons of benzene are evident in the current density maps:[9,12] they also could generate proton deshielding.

In any event, the π-flow is, to a substantial extent, responsible for the downfield chemical shift observed in proton magnetic resonance, by deshielding the perpendicular component σ_{33} via a local mechanism.[35]

Table 5. CTOCD-CHF Principal Values of the ^1H Magnetic Shielding Tensors in Anthracene[a]

hydrogen	DZ2	PZ2	exp.
H_1			
σ_{11}	28.8	29.5	
σ_{22}	23.5	24.0	
σ_{33}	17.8	17.9	
σ_{av}	23.4	23.8	22.92[b], 22.91−23.02[c]
H_2			
σ_{11}	27.9	28.3	
σ_{22}	24.6	25.0	
σ_{33}	19.9	20.0	
σ_{av}	24.1	24.4	23.44[b], 23.45−23.56[c]
H_9			
σ_{11}	29.4	30.2	
σ_{22}	23.4	23.7	
σ_{33}	15.7	15.7	
σ_{av}	22.8	23.2	22.52[b], 22.48−22.59[c]

[a] In ppm. See text for geometry and basis set. Hydrogens are numbered as the carbons to which are bonded. Absolute experimental shieldings have been obtained from the shifts reported in [b]ref 39, using $\delta_H(CH_4) = 0.22$ and $\sigma_H(CH_4) = 30.61$, and from the chemical shifts with respect to benzene measured in [c]ref 40, using the absolute $\sigma_H(C_6H_6) = 23.57-23.68$ estimated in ref 18.

Table 6. CTOCD-CHF Principal Values of the ^1H Magnetic Shielding Tensors in Phenanthrene[a]

hydrogen	DZ2	PZ2	exp.
H_1			
σ_{11}	28.7	29.2	
σ_{22}	23.7	24.2	
σ_{33}	18.3	18.4	
σ_{av}	23.6	23.9	22.83−23.40[b], 23.04−23.15[c]
H_2			
σ_{11}	27.5	27.8	
σ_{22}	24.4	25.0	
σ_{33}	19.9	19.9	
σ_{av}	23.9	24.2	22.83−23.40[b], 23.33−23.44[c]
H_3			
σ_{11}	27.8	28.2	
σ_{22}	24.4	25.0	
σ_{33}	19.4	19.5	
σ_{av}	23.9	24.2	22.83−23.40[b], 23.27−23.38[c]
H_4			
σ_{11}	29.5	30.4	
σ_{22}	22.9	23.3	
σ_{33}	15.5	15.6	
σ_{av}	22.6	23.1	22.12[b], 22.22−22.33[c]
H_9			
σ_{11}	28.8	29.1	
σ_{22}	24.0	24.5	
σ_{33}	18.1	18.4	
σ_{av}	23.6	24.0	23.12[b], 23.19−23.30[c]

[a] See footnote to Table 5.

The superposition of internal and peripheral electron circulations observed for anthracene in Figure 1 should cause sizable additional deshielding of σ_{33} of proton H_9. As a matter of fact, its theoretical value, 15.7 ppm, is 2.1 smaller than σ_{33} evaluated for H_1, and 4.2 smaller than that of H_2, see Table 5. However, the map does not provide any tool to explain why σ_{33} of H_2 is 2.1 ppm larger than that of H_1. A similar trend had been found in naphthalene molecule,[16] where CTOCD theoretical values for σ_{33} range in the interval 18.1−18.6 and 19.6−20.2 ppm for H_1 and H_2, respectively. Also in phenanthrene and triphenylene σ_{33} of H_1 is smaller than that of H_2 (see Tables 6 and 7). The delocalized π-electron current does not seem responsible for these differences, as it flows all over the peripheral carbon path appreciably with the same intensity; analysis of the σ-electron contributions is necessary to assess their role. In any event, the maps for naphthalene actually reveal quite different phase

(34) Iuliucci, R. J.; Phung, C. G.; Facelli, J. C.; Grant, D. M. *J. Am. Chem. Soc.* **1998**, *120*, 9305−9311.
(35) Lazzeretti, P.; Zanasi, R. *Chem. Phys. Lett.* **1983**, *100*, 67−69.
(36) Lide, D. R., Ed.; *Handbook of Chemistry and Physics*, 74th ed.; CRC Press: Boca Raton, 1993−1994.
(37) Breitmaier, E.; Haas, G.; Voelter, W. *Atlas of Carbon-13 NMR Data*; Heyden: London, 1979.
(38) Jameson, A. K.; Jameson, C. J. *Chem. Phys. Lett.* **1987**, *134*, 461−466.
(39) Jonathan, N.; Sidney, G.; Dailey, B. P. *J. Chem. Phys.* **1962**, *36*, 2443−2448.
(40) Haigh, C. W.; Mallion, R. B. *Mol. Phys.* **1971**, *18*, 737−751.

Table 7. CTOCD-CHF Principal Values of the ^{1}H Magnetic Shielding Tensors in Triphenylene[a]

hydrogen	DZ2	PZ2	exp.
H_1			
σ_{11}	29.8	30.4	
σ_{22}	22.8	23.3	
σ_{33}	15.3	15.5	
σ_{av}	22.6	23.1	22.27[b], 22.23−22.34[c]
H_2			
σ_{11}	27.7	28.1	
σ_{22}	24.5	25.0	
σ_{33}	19.5	19.6	
σ_{av}	23.9	24.2	23.22[b], 23.26−23.37[c]

[a] See footnote to Table 5.

portraits;[16] a focus is observed close to H_1, whereas a toroidal circulation is found in the region of H_2. These features seem to confirm the hypothesis of the relevance of σ-electrons at least qualitatively. As regards the comparison between theoretical and experimental data, it can be seen that, as far as the average proton shielding is concerned, the latter is systematically lower than either DZ2 or PZ2 estimates, even if, in most cases, the difference is a fraction of ppm.

Conclusions

We have presented ab initio π-electron first-order current density maps and second-order magnetic properties, calculated at the SCF/CHF level of approximation, for a series of polycyclic aromatic hydrocarbons. Thanks to the use of a distributed-origin method, the computed magnetic properties are generally in very good agreement with the available experimental data.

We conclude that the current density maps shown here yield accurate descriptions of the actual π-electron flow induced by an external, uniform magnetic field in these systems and outline a pattern that may occurr also in higher homologous molecules. The features shown for the first time in these maps cannot be deduced on the basis of the very simple RCM.

Eventually, we have shown the power of CTOCD methods for theoretical determination of quantities that are fundamental to interpret molecular magnetic response, that is, principal values of magnetizability and nuclear magnetic shielding tensors. It is worth emphasizing that these calculations can be routinely carried out at a very low cost for large molecular systems.

Acknowledgment. Financial support from the Italian Ministero dell'Università e della Ricerca Scientifica e Tecnologica (MURST), via 40% and 60% funds, and from the Italian Consiglio Nazionale delle Ricerche (CNR)-Commitato Chimica, is gratefully acknowledged.

JA9900656